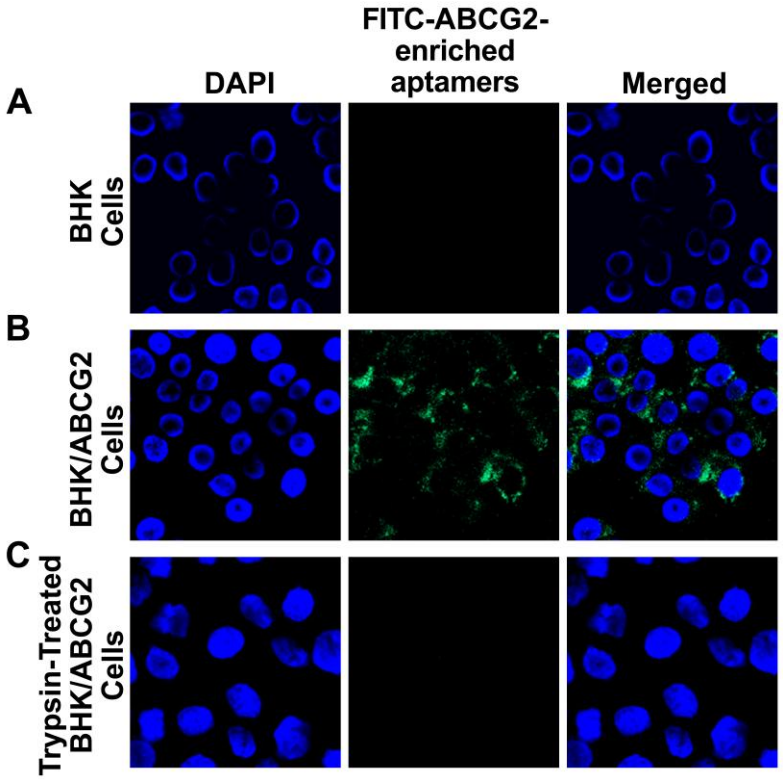

Figure S1: The ABCG2-enriched (after 15 cycles of binding and counter-selection) aptamers can bind to the ABCG2-expressing BHK/ABCG2 cells. A. The ABCG2-enriched aptamers cannot bind to the parental BHK cells: left section, cells were stained with DAPI; middle section, with FITC-labeled ABCG2-enriched aptamers; right section, merge of the previous two sections. B. The ABCG2-enriched aptamers can bind to the surface of the ABCG2-expressing BHK/ABCG2 cells. C. Short time trypsin digestion completely abolished the staining of BHK/ABCG2 cells with the ABCG2-enriched aptamers.

Figure S2: Nucleotide sequence of the cloned ABCG2-specific aptamer ABCG2/A12.
5'-ACGCTCGGATGCCACTACAGGCCCACCCTCATGGACGTGCTGGTGAC-3'

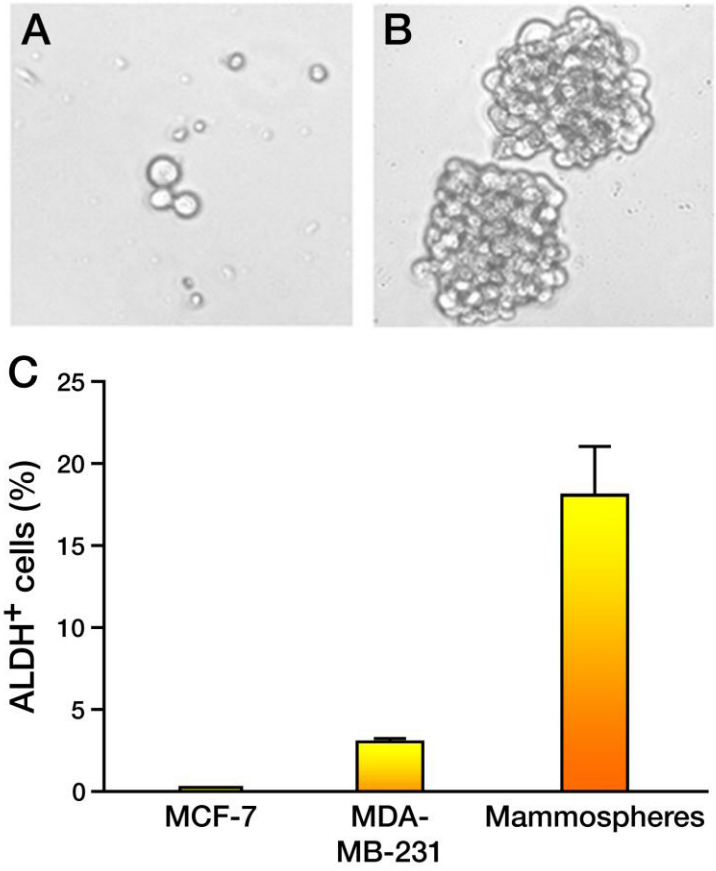

Figure S3: ALDH$^-$ cells cannot form mammospheres (A), whereas ALDH$^+$ cells can (B). (C) The percentage of ALDH$^+$ cells in mammospheres derived from MCF-7 is significantly higher than in MCF-7 cell line or in MDA-MB-231 cell line.

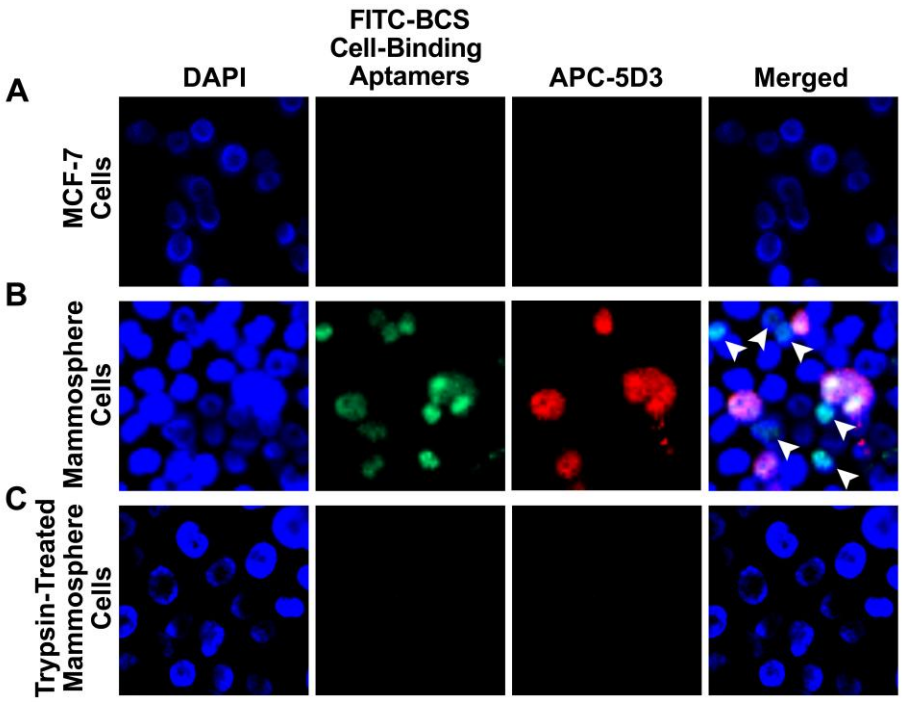

Figure S4: The BCS cell-enriched (after 15 cycles of binding and counter-selection) aptamers can bind to some of the mammosphere cells derived from MCF-7. A. BCS cell-enriched aptamers cannot bind to the differentiated breast cancer MCF-7 cells: left section, cells were stained with DAPI; second section, with FITC-labeled BCS cell-enriched aptamers; third section, with APC-conjugated human ABCG2-specific mAb 5D3; right section, merge of the previous three sections. B. BCS cell-enriched aptamers detected more mammosphere cells than the human ABCG2-specific mAb 5D3. Arrowheads indicate the cells detected by the BCS cell-enriched aptamers, but not by ABCG2-specific mAb 5D3. C. Short time trypsin digestion completely abolished the staining of the cells derived from mammospheres with the BCS cell-enriched aptamers and the ABCG2-specific mAb 5D3.

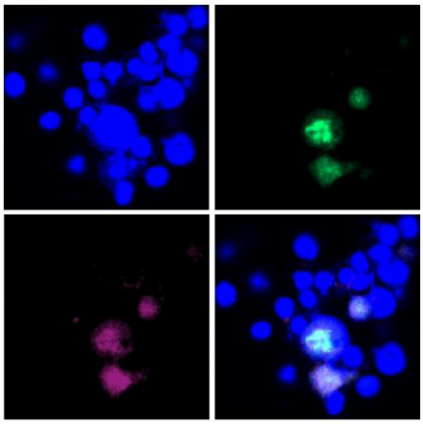

Figure S5: The BCS cell-enriched (after 15th cycle of binding and counter-selection) aptamers detected CD44-expressing BCS cells. Top left, mammosphere cells derived from human fresh breast cancer specimen were stained with DAPI; top right, with FITC-labeled BCS cell-enriched aptamers; bottom left, with APC-conjugated anti-CD44 mAb; bottom right, merge of the previous three sections.

Figure S6: Nucleotide sequence of the cloned BCS cell-binding aptamer BCS/A35.

5'-ACGCTCGGATGCCACTACAGATCGCCCCTCACCTCATGGACGTGCTGGTGAC-3'

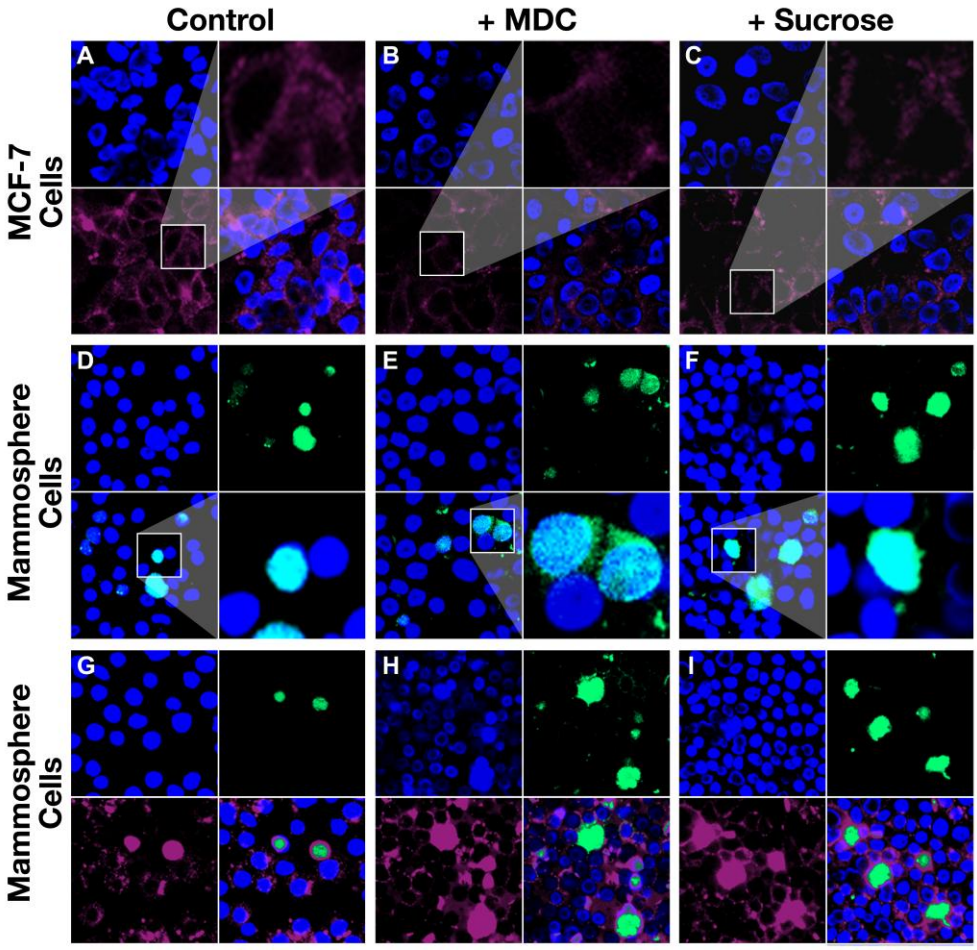

Figure S7: BCS cells have a significantly higher rate of clathrin-independent endocytosis than the differentiated breast cancer cells. A. Staining of the differentiated breast cancer MCF-7 cells with hTF in the absence of CDE inhibitor: top left, cells were stained with DAPI; bottom left, with Alexa fluor 633-conjugated hTF; top right, amplified image of the cells from bottom left section; bottom right, merge of the top left section and bottom left section. B. Staining of the differentiated breast cancer MCF-7 cells with hTF in the presence of CDE inhibitor MDC. C. Staining of the differentiated breast cancer MCF-7 cells with hTF in the presence of CDE inhibitor sucrose. D. Staining of the mammosphere cells derived from MCF-7 with ABCG2/A12 in the absence of CDE inhibitor: top left, cells were stained with DAPI; top right, with FITC-labeled ABCG2/A12; bottom left, merge of the top left section and bottom left section; bottom right, amplified image of the cells from bottom left section. E. Staining of the cells derived from mammospheres with ABCG2/A12 in the presence of CDE inhibitor MDC. F. Staining of the cells derived from mammospheres with ABCG2/A12 in the presence of CDE inhibitor sucrose. G. Co-staining of the cells derived from mammospheres with ABCG2/A12 and hTF in the absence of CDE inhibitor: top left, cells were stained with DAPI; top right, with FITC-labeled ABCG2/A12; bottom left, with Alexa fluor 633-conjugated hTF; bottom right, merge of the previous three sections. H. Co-staining of the cells derived from mammospheres with ABCG2/A12 and hTF in the presence of CDE inhibitor MDC. I. Co-staining of the cells derived from mammospheres with ABCG2/A12 and hTF in the presence of CDE inhibitor sucrose.

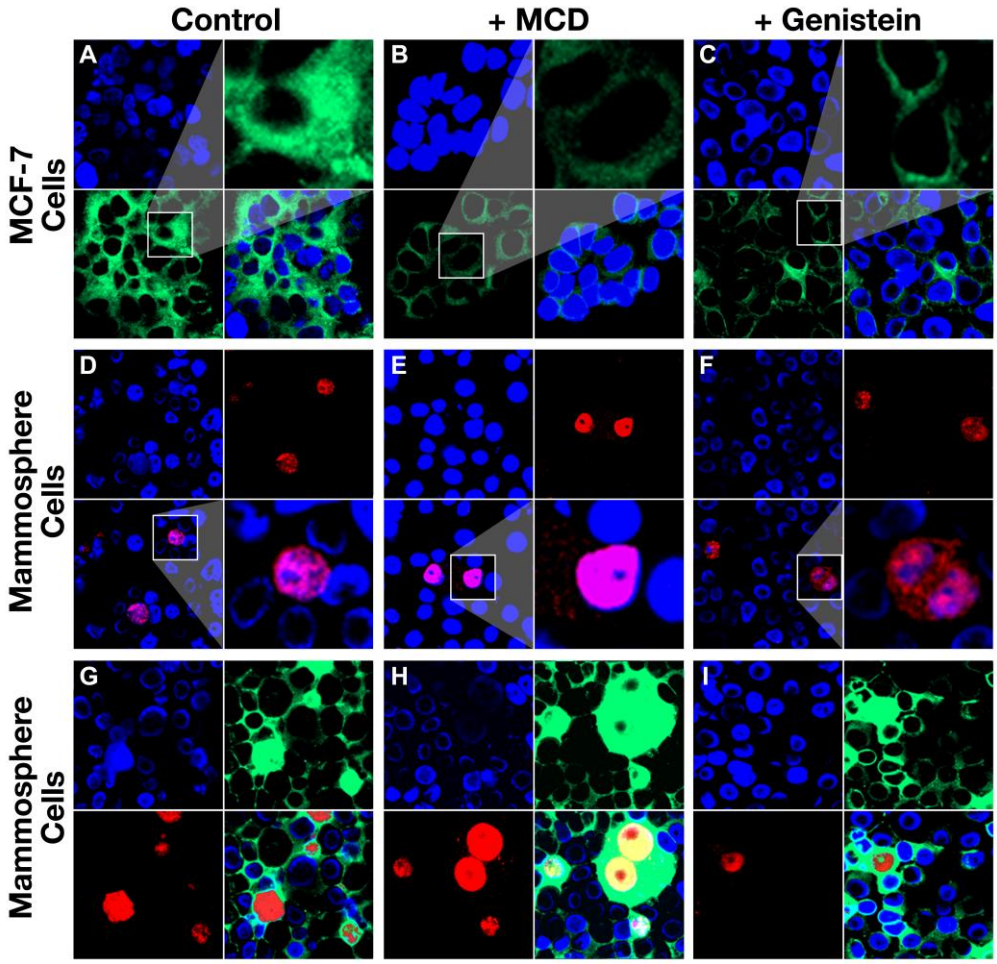

Figure S8: BCS cells have a significantly higher caveolin-independent endocytosis than the differentiated breast cancer cells. A. Staining of the differentiated breast cancer MCF-7 cells with LacCer in the absence of CVDE inhibitor: top left, cells were stained with DAPI; bottom left, with BODIPY-labeled LacCer: top right, amplified image of the cells from bottom left section; bottom right, merge of the top left section and bottom left section. B. Staining of the differentiated breast cancer MCF-7 cells with LacCer in the presence of CVDE inhibitor MCD. C. Staining of the differentiated breast cancer MCF-7 cells with LacCer in the presence of CVDE inhibitor genistein. D. Staining of the mammosphere cells derived from MCF-7 with ABCG2/A12 in the absence of CVDE inhibitor: top left, cells were stained with DAPI; top right, with TR-labeled ABCG2/A12; bottom left, merge of the top left section and top right section; bottom right, amplified image of the cells from bottom left section. E. Staining of the cells derived from mammospheres with ABCG2/A12 in the presence of CVDE inhibitor MCD. F. Staining of the cells derived from mammospheres with ABCG2/A12 in the presence of CVDE inhibitor genistein. G. Co-staining of the cells derived from mammospheres with ABCG2/A12 and LacCer in the absence of CVDE inhibitor: top left, cells were stained with DAPI; top right, with BODIPY-labeled LacCer; bottom left, with TR-labeled ABCG2/A12; bottom right, merge of the previous three sections. H. Co-staining of the cells derived from mammospheres with ABCG2/A12 and LacCer in the presence of CVDE inhibitor MCD. I. Co-staining of the cells derived from mammospheres with ABCG2/A12 and LacCer in the presence of CVDE inhibitor genistein.